Published by
NIGERIAN SOCIETY OF PHYSICAL SCIENCES
Available online @ https://journal.nsps.org.ng/index.php/jnsps

J. Nig. Soc. Phys. Sci. 8 (2026) 2604

Journal of the Nigerian Society of Physical Sciences

Multi-proxy evidence from the exposed strata at Okpekpe, Imiegba, and environs for nomenclature as Mamu Formation, Benin Flank, NW Anambra basin, Nigeria

Israel Aruoriwo Abiodun Etobro*, Omabehere Innocent Ejeh

Department of Geology, Delta State University, Abraka, Nigeria

Abstract

Litho-sections along Okpekpe, Imiegba, and environs have been studied for their textural and microfossil contents to elucidate this recently exposed lithostratigraphic unit in the Benin Flank of the Anambra Basin. Five of the road-cut sections were mapped for their textural characteristics, facies types and associations, and palynostratigraphy to decipher their age, and palaeoenvironment, for proper assignment to a lithostratigraphic unit. Facies analysis reveals four facies types namely: shale, sandstone, mudstone, and coal facies. The mudstone facies is characterised by abundant *Thalassinoides* ichnogenus that suggest a deposition under littoral environment. Index palynomorphs markers: *Trichodinum lasstaneum*, *Andahisiella polymorpha*, *Cingulatisporites ornatus*, *Dinogymnium* sp., *Cerodinium diebelii*, *Buttinea andreevi, Cyclonephelium* sp., *Laevigatosporites major, Odontochitina operculata*, and *Longapertites marginatus*, recovered from both the shale and mudstone facies revealed Early Maastrichtian age. The sandstone facies is coarse-grained, poorly-sorted, nearly symmetrical, mesokurtic sandstone. Bivariate plots, linear discriminant and multivariant functions revealed deposition in a range of depositional environments, including shallow marine, beach, and fluvial environments. The combination of facies association and the microfossils suggests a transition between non-marine and marine environments for the exposed litho-sections. The facies types and associations, age, and palaeoenvironment revealed by the exposed sections correlate with the Mamu Formation, suggesting that this lithostratigraphic unit is not restricted to the eastern part of the Anambra basin but also in the Benin Flank.

DOI:10.46481/jnsps.2026.2604

Keywords: Dinoflagellates, Mamu formation, *Thalassinoides*, Age dating

Article History :
Received: 01 January 2025
Received in revised form: 05 June 2025
Accepted for publication: 06 June 2025
Published: 28 February 2026

Communicated by: Oladiran Johnson Abimbola

1. Introduction

The Anambra Basin is an extensive, triangular-shaped sedimentary basin in southern Nigeria [1–3]. Existing literature revealed that the basin has been widely studied by many authors [1, 2, 4–15]. Most of these studies, however, covered the main axis and central part of the basin in southeastern Nigeria, whereas its northwestern flank (Benin Flank) has only attracted limited attention [12, 16–20]. Although the flanks of sedimentary basins are generally known to comprise relatively thin and younger lithostratigraphic units owing to the usual basin geometry that often portrays stratal shallowing away from the basin

*Corresponding author: Tel. No.: +234-816-278-4767.
Email address: aaietobro@delsu.edu.ng (Israel Aruoriwo Abiodun Etobro)

centre, the Benin Flank has been reported by Ejeh *et al*. [14] to have a sedimentary fill of approximately 1000 m (depth to basement); however, in this study, its recent exposures will be investigated. Also, despite the numerous studies on the stratigraphic and palaeontologic aspects of the southern sedimentary basins of Nigeria (Anambra Basin inclusive), Kogbe [21] stated that unresolved controversies about the stratigraphy, especially in terms of nomenclature, type sections/locality, spacio-temporal extent, and superposition/relative age still exist. For example, before the recent sedimentary exposures due to roads constructed in Imiegba, Okpekpe and environs, the Ajali Formation was thought to be the main lithostratigraphic unit outcropping in the Benin Flank of the basin; while the older stratigraphic unit, the Mamu Formation was hitherto thought by some authors [1, 2, 21–24] to have terminated at Idah (located on the eastern part of the River Niger). The new roads constructed in Imiegba-Okpekpe areas have exposed the older strata, which were mapped and related to the lithofacies of the Mamu Formation [12, 18].

However, Adebayo *et al*. [17] referred to these strata as the Nkporo Formation. It is therefore necessary to validate which lithostratigraphic unit the newly exposed strata. The present study intends to ascertain the lithostratigraphic unit of the exposed strata at Imiegba-Okpekpe area in terms of relative age and palaeoenvironment through lithofacies analysis and palynostratigraphic examination in comparison to the main/similar stratigraphic unit in the eastern part of the basin.

2. Regional geology of the Anambra basin

The Anambra Basin is thought as a NE-SW trending Cretaceous sedimentary basin with its flanks lying to the northwestern and southeastern (Figures 1(a) and 1(b)). The northwestern flank is referred to as the Benin Flank. The Anambra Basin is stratigraphically composed of Late Cretaceous to Cenozoic sediments (Figure 2). However, the proto-Anambra Basin comprises older sediments of the Early Cretaceous that were affected by the Santonian contractional deformation event. The deformation event led to the subsequent folding of the pre-Santonian sediments [1, 3]. The proto-Anambra Basin is made up of the folded Asu River Group, the Eze-Aku Formation, and the Awgu Shale. The post-Santonian lithostratigraphic units include the Nkporo Shale, the Mamu Formation, the Ajali Formation, the Nsukka Formation, the Imo Shale, the Ameki Group/Nanka Formation and the Ogwashi-Asaba Formation (Figure 2). The environments of deposition varied from non-marine, through transitional, to marine with the accumulation of Cretaceous and Cenozoic sediments. The marine incursion that occurred during the Coniacian was represented by the Awgu Shale [2].

The Mamu Formation has been studied by many authors [5, 6, 9, 12–14, 23]. In southeastern Nigeria, this formation consists of a sequence of sandstone, mudstone, shale, sandy shale, and coal seams [21–23]. The rock sequence has variable thicknesses but is generally thickest at the basin centre. According to Refs. [5, 6, 9, 14, 22], the associated coal seams have attracted research interests throughout the past decades. The coal seams have variable thicknesses and their occurrences have led earlier authors to tag the Mamu Formation as the Lower Coal Measure in the basin centre [23]. The Maastrichtian age has been assigned to the Mamu Formation and the sandstone was described to be deposited in a low-saline fresh water environment, while the ammoniferous shale was deposited in the marine environment [2, 21, 23]. The environment of deposition for the Mamu Formation was generally transitional between the non-marine and marine environments [2, 13, 14, 23].

3. Materials and methods

The present study involved mapping the exposed strata at Okpekpe, Imiegba, and the surrounding areas lying between Latitudes 7° 9′ 00″ to 7° 15′ 00″N and Longitudes 6° 25′ 00″ to 6° 30′ 00″ E (Figure 1c). Outcrop samples (no. = 30) obtained during a detailed mapping exercise of the exposed stratigraphy were used for this study. Detailed lithostratigraphic descriptions were carried out on five (5) road-cut sections following international standard by considering facies types and association, textural characteristics (grain-size, shape, and fabric), colour, mineralogical composition, sedimentary structures, ichno-fossil and macrofossil contents, post-depositional effects (i.e., diagenesis) and geometry [28]. Fresh sandstone and shale samples were obtained alongside their geographical locations using the Global Positioning System (GPS). The sandstone samples were subjected to grain-size analysis and heavy mineral separation analysis, while the shale units were subject to microfossil analysis to extract palynomorphs. This involved facies analysis and the extraction of palynomorphs (Dinoflagellates, Spores, and Pollen) from the interbedded shale and mudstone lithologic unis. Facies association and inferred age obtained from the palynomorphs were regionally correlated with those of the established ages of the lithostratigraphic units occurring in the basin centre to ascertain a lithostratigraphic unit [1, 23].

3.1. Grain-size analysis

Fifteen (15) fresh sandstone samples were chosen for the grain-size analysis to determine their textural characteristics. The samples selected were most suitable because they are fresh and not weathered. The mechanical sieving method using a Rotap sieve shaker was adopted. Each sample was gently disaggregated using a mortar and pestle, ensuring individual grains were neither crushed nor broken. 100 g of each sample was measured out after coning and quartering and poured into a set of sieves (of 1/2ϕ intervals) arranged in decreasing mesh size downwards. Each sample was mechanically shaken for 15 minutes. The weight retained in each sieve was recorded against its mesh size. The weight percent and cumulative weight percent retained in each sieve and the pan were computed and tabulated. Plots of frequency and cumulative frequency curves were drawn for all the sieved samples. Statistical parameters including graphic mean, standard deviation, inclusive skewness and kurtosis were computed and interpreted for each sample using formulas and standard tables proposed by Folk and Ward [29].

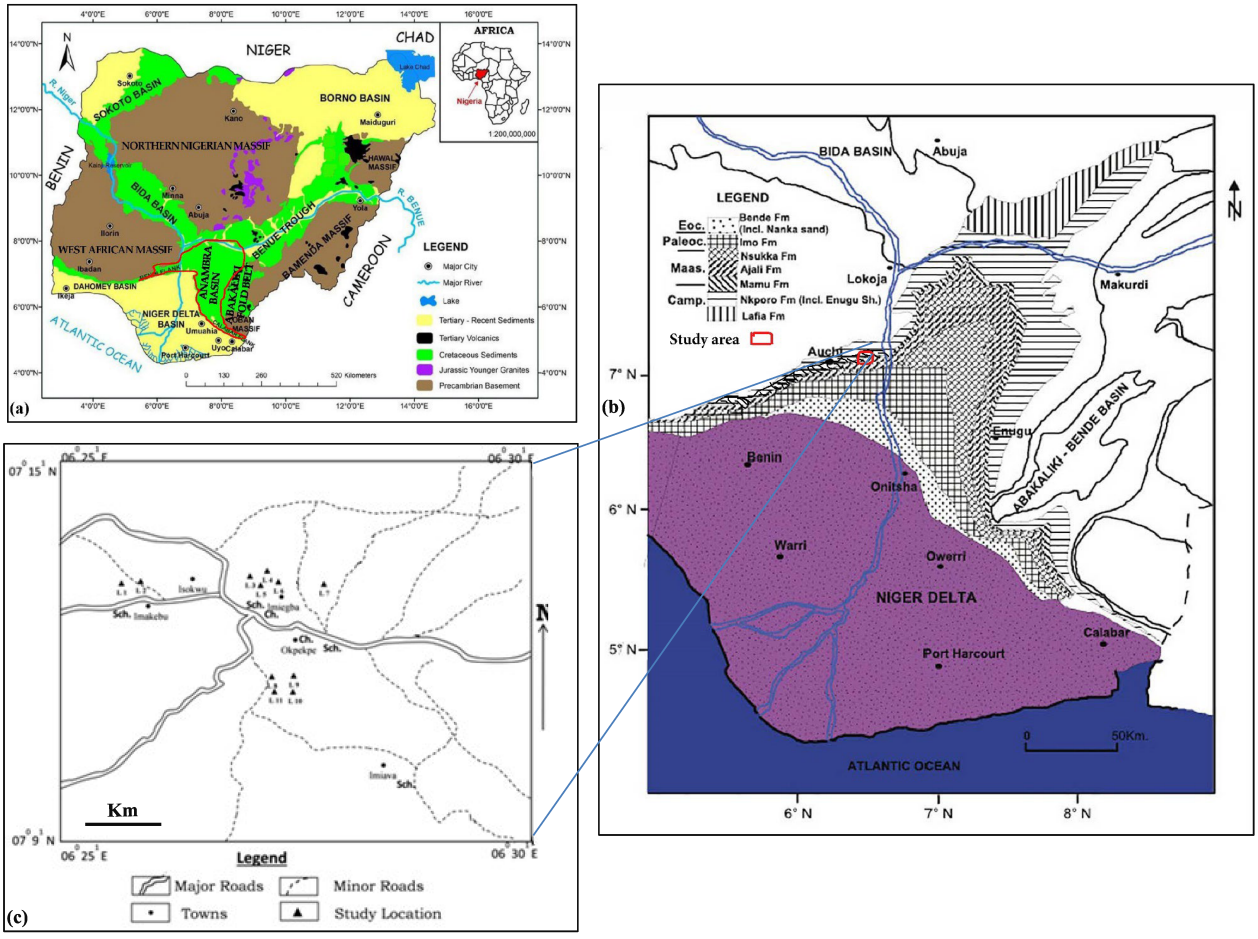

Figure 1. (a) Outline Geological map of Nigeria with Anambra Basin indicated (modified after Lar *et al.* [25]. (b) Geological map of Anambra Basin (after Refs. [4, 26], modified after Ogungbesan and Adedosu [27]. (c) Map of the study area/sample locations.

3.1.1. Discriminatory analyses

Further treatment of grain size textural parameters includes linear discriminant function (LDF) and multivariant discriminant function (MDF) of Sahu [31] and of Sahu [30] respectively. Such discriminant function analyses have been applied by Etobro *et al.* [32] for sedimentary depositional environmental discrimination between certain pairs of depositional settings (e.g., shallow agitated marine and beach; shallow marine and fluvial). The linear discriminant function was applied for the sandstone facies of the Mamu Formation following the equations (1) to (4) proposed by Sahu [31]:

Y_1 Aeolian process vs Beach (littoral) =

$$-3.5688Mz + 3.7016\sigma^2 - 2.0766Sk_1 + 3.1135KG, \quad (1)$$

Y_2 Beach vs shallow agitated marine =

$$15.6534Mz + 65.7091\sigma^2 + 18.1071Sk_1 + 18.5043KG, \quad (2)$$

Y_3 Shallow marine vs fluvial processes =

$$0.2852Mz - 8.7604\sigma^2 - 4.8932Sk_1 + 0.0482KG, \quad (3)$$

Y_4 Fluvial (deltaic) vs turbidity current deposition =

$$0.7215Mz - 0.40306\sigma^2 + 6.7322Sk_1 + 5.2927KG, \quad (4)$$

where: Mz = Graphic mean size; σ = Standard deviation; Sk_1 = Graphic inclusive skewness; and KG = Graphic kurtosis

$Y_1 < -2.7411$ would show aeolian deposition; and > -2.7411 would indicate beach environment, $Y_2 < 65.3650$ would show beach deposition; and > 65.3650 would indicate beach deposition, $Y_3 < -7.4190$ would show fluvial (deltaic) deposit; and > -7.4190 would indicate shallow marine deposit and; $Y_4 < 9.8433$ would show turbidity current deposition, and > 9.8433 would indicate fluvial (deltaic) deposition. Another

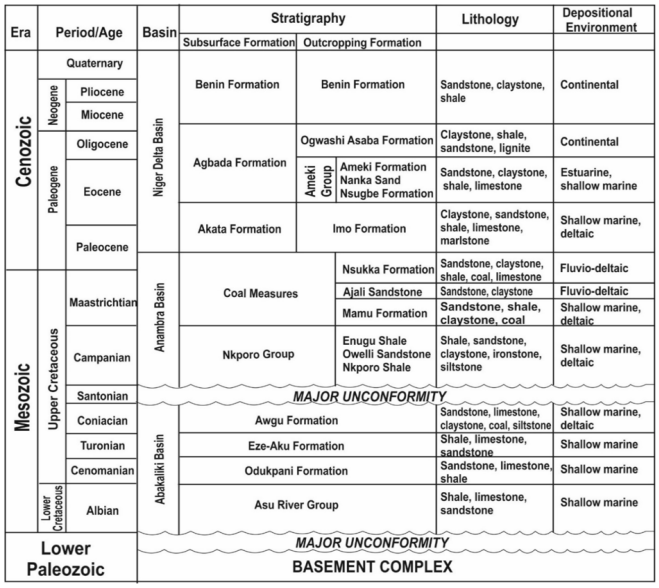

Figure 2. Stratigraphic succession in the southern Nigeria sedimentary basins (after [23]).

Facies	Sub-facies	Lithology/outcrop photo	Lithologic Description	Environment of Deposition
Sandstone	Ferruginised sandstone		Grey to reddish black; highly indurated	Non-marine
	Non-ferruginised sandstone		Whitish sands with occasional thin shale interbeds (heteroliths)	Fluvial
Coal	Lignite		Black coal seam, thinly bedded with shale	Swamp
Mudstone	Mudstone		White, interbedded with shale	Beach?
	Burrowed Mudstone		Grey, numerous burrows Thallasinoides)	Littoral
Shale	Carbonaceous shale (fissile)	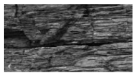	Dark grey to black; intercalations with mudstone are common	Shallow marine

Figure 3. Facies associations of the Mamu Formation observed at the study area (Okpekpe, Imiegba, and surrounding areas).

discriminant function method applied in this study is the multivariant discriminant function analysis of Sahu [30] with the following equations (5) and (6):

$$\tilde{V}_1 = 0.48048Mz + 0.06231\sigma^2 + 0.40602Sk_1 + 0.44413KG, \quad (5)$$

and

$$\tilde{V}_2 = 0.24523Mz + 0.45905\sigma^2 + 0.15715Sk_1 + 0.83931KG, \quad (6)$$

where V_1 = Eigen vector 1, and V_2 = Eigen vector 2.

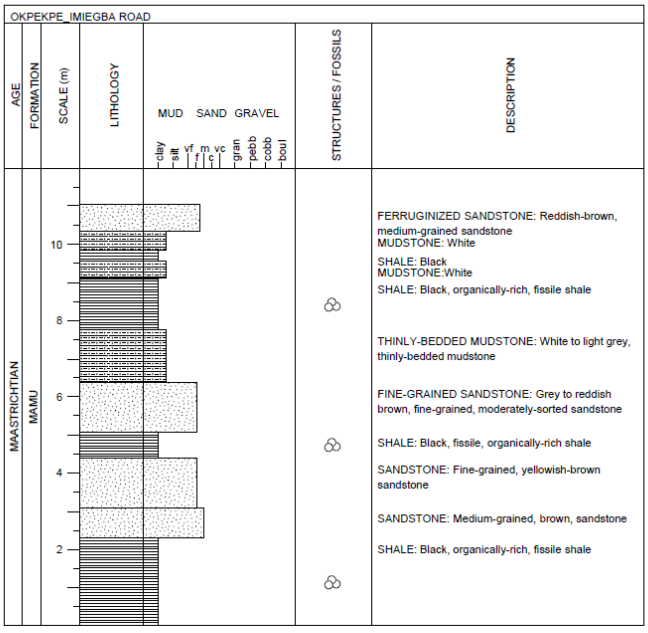

Figure 4. Graphic lithologic section of the Mamu Formation observed at Okpekpe and Imiegba road-cuts with varying lithofacies, including shale, mudstone, and sandstone. Note the alternation of the sandstone and shale/mudstone.

3.2. *Microfossil analysis*

Six (6) shale samples were chosen for the microfossil analysis. The shale samples chosen are most suitable for fossil analyses due to their fresh state, and abundant microfossils can be recovered from even small sample sizes. The selected samples were decarbonised with 10% dilute hydrochloric acid (HCl) to remove calcareous materials. This was followed by maceration with 60% hydrofluoric acid (HF) overnight to remove the silicate minerals. A 5 mm nylon mesh was used to sieve the digested samples to improve palynomorph recovery and to achieve the best slides for microscope view. The retrieved sample residue was mildly oxidised with nitric acid (HNO_3), neutralised with potassium hydroxide (KOH), and followed by heavy mineral liquid separation of the macerals using zinc bromide ($ZnBr_2$) at 2.1 g/ml. The collected residue was mounted on two glass slides per sample using DPX mounting medium. Quantitative absolute counts of encountered taxa were recorded while important index markers, including pollen and spores, were photographed with the *Nikon CoolPix P6000* digital camera.

4. Results and discussions

4.1. *Geology of the study area (Okpekpe, Imiegba, and surrounding areas)*

The geological mapping exercise revealed that the study area comprises a sequence of shale, mudstone, sandstone, and coal facies (Figure 3). The entire rock sequence exposed by the road cuts in the study area varies in thickness from about 5 to 14 m (Figures 3 and 4).

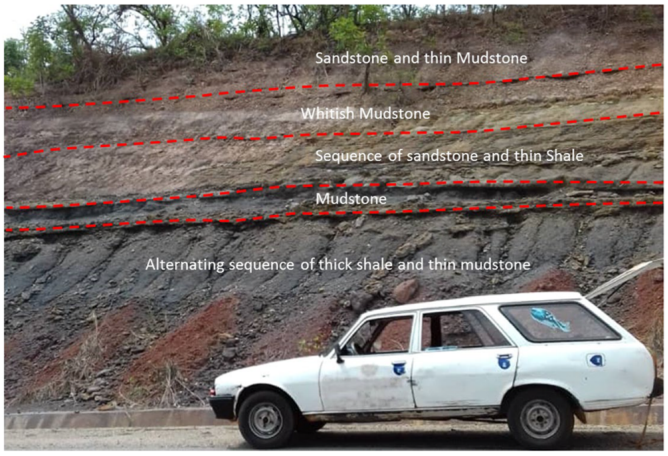

Figure 5. Road-cut section showing the sedimentary rock sequences. Note the thick shale at the base with some intercalation of thin mudstone. The car for scale in the picture is 1.46 m high and 4.8 m long.

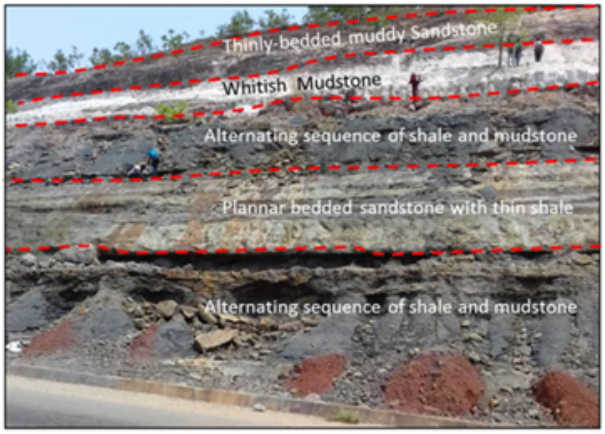

Figure 6. Road-cut section showing the thick shale comprising some intercalations of thin mudstone. The thickness of the interbedded mudstone increases upwards while the thickness of the shale decreases upward. The person for scale on the whitish mudstone is 1.6 m tall.

4.1.1. *Shale facies*

The shale facies consists of grey to black coloured types, fissile with thin shale laminae (4 to 15 mm thick), and occasionally interbedded with mudstone and sandstone. The thickness of the interbedded mudstone increases upwards while the shale thins upwards. Laminations are important sedimentary structures associated with this shale facies. The laminations are continuous and conspicuous, although occasionally non-continuous in some localities. The thickness of the exposed shale varies from 5 cm to 2 m (Figure 5).

4.1.2. *Mudstone facies*

The mudstone facies varies from white, creamy, brown, and light grey, and is characteristically fine textured, with varying silty and clayey particles. It consists of both mudstone and burrowed mudstone sub-facies (Figure 5). The mudstone sub-facies is more common in the study area, occurring as interbeds with sandstone and shale in the studied sections (Figures 5 and 6).

Burrowed mudstone sub-facies

The burrowed light brown sub-facies is (Figure 7) affected by bioturbation processes by a group of trace fossils, *Thalassinoides* ichnogenus (Figure 7c). The burrow traces are a colony of vertical, mostly horizontal, or branching traces (Figures 7c and 7d). Some of the burrow traces are filled, while others are unfilled. The burrow traces diameter is variable, and generally less than 1 cm in diameter. The concentration of the burrow traces suggests sedimentation under an aerobic bottom condition whereby organism thrived on the deposited sediment in search of food. The burrowed mudstone sub-facies unit ranges from 15 to 35 cm thick.

4.1.3. *Coal facies*

This facies is composed of black coal (Figure 8) that lacks lamination or graded beddings. The thickness of the coal facies is about 15 cm. The coal facies is localized in the study area and it occurs as an interbedded unit with the shale facies. Coal has been described by many researchers as one of the facies associations of the Mamu Formation in most parts of the Anambra Basin [13, 18, 23].

4.1.4. *Sandstone facies*

The whitish, reddish-brown, to brownish sandstone facies varies in grain size from medium- to coarse-grained. The sandstone facies occurs as planar bedded with a thickness of 8 to 30 cm. There are two varieties of the sandstone facies, namely the non-ferruginised and ferruginised sandstone sub-facies.

Non-ferruginised sandstone sub-facies

It is often interbedded with thin layers of shale and occasionally mudstone. The sandstone facies is indurated, consisting of mineral grains including quartz, feldspar, and mica. The particle shape ranges from sub-angular to rounded, and their sorting varies from poorly to moderately-sorted.

Ferruginised sandstone sub-facies

The ferruginised sandstone sub-facies is generally more indurated than the non-ferruginised sandstone sub-facies. It is reddish brown and sometimes grey. Mineral grains include quartz, feldspar, and iron-rich minerals acting as cement, hence their dark colour. The ferruginised sandstone is characterised by fine to medium texture. It occasionally occurs as capping the entire studied lithostratigraphic unit in the study area.

4.2. *Textural characteristics and source area of the clastic sediments*

Cumulative frequency curves were plotted on a metric graph for the statistical parameters (graphic mean, standard deviation, inclusive skewness, and kurtosis) computation. The grain-size analysis of the interbedded sandstone facies shows

that it is composed of fine- to coarse-grained (av. medium-grained), very poorly-sorted to very well-sorted (av. poorly-sorted), fine- to coarse-skewed (av. nearly symmetrical), very platykurtic to very leptokurtic (av. leptokurtic) sandstone (Table 1). The dominant poorly sorting of the sandstone facies suggests deposition in a fluvial environment [28, 33, 34]. The dominant fine to coarse grains that characterized the sandstone facies is indicative of a relatively high-energy medium responsible for their deposition. Such high energy may be likened to that associated with the high-energy fluvial body, such as a fast-flowing river.

4.3. Biostratigraphy

The analysed six (6) shale samples indicate species association of Palynomorphs comprising species of Dinoflagellates, Spores, Pollens, and some Foraminiferal linings.

4.3.1. Quantitative Dinoflagellate cyst distribution

Thirty-five (n = 35) different species of Dinoflagellate cysts, consisting of 472 individuals, were recovered from the six analysed samples (Table 2, Figure 9). The species population of the Dinoflagellates extracted from sample Img1 is 145, which makes 33 different species (Table 2, Figures 10 and 11). They show variable species abundance and species diversity; however, two of the analysed samples (i.e., Img1 and S9) display both high species diversity and abundance. Species abundance is recorded by the following Dinoflagellate species: *Cerodinium obliquipes* (29), *Areoligera coronate* (27), *Trichodinium castaneum* (23), *Cyclonephelium sp.* (22), *Palaeohystrichophora infusoroides* (21), and *Andalusiella polymorpha* (20) (Table 2).

4.3.2. Quantitative distribution of the Spores and Pollens

Twenty-eight (n = 28) species of Spores and Pollens (Figure 12) comprising 489 populations were extracted from the six analysed samples. Samples Img1 and S9 also show species diversity and population of the Spores and Pollens. Sample Img1 is composed of 27 different species comprising 175 populations, while Sample S9 is made up of 24 species types (Figures 13 and 14) and 114 populations (Table 3). High species populations are observed among the following spores and pollens: *Leiotriletes adriennis* (45), *Psilamonocopites sp.* (40), *Matonisporites equiexinus* (33), *Longapertites marginatus* (33), *Laevigatosporites discordatus* (31), *Laevigatosporites major* (29), *Echitriporites trianguliformis* (28), and *Cyathidites australis* (28) (Table 3).

4.3.3. Age determination

Species of Dinoflagellate, Spores, and Pollens were used for the relative age determinations of the exposed sections. Most of the analysed samples allow a correlation with either Late Campanian or Early Maastrichtian biozones (Table 4). However, some index organic-walled microfossils of Early Maastrichtian age have been recovered namely: *Trichodinum lasstaneum, Andahisiella polymorpha, Cingulatisporites ornatus, Dinogymnium sp., Cerodinium diebelii, Buttinea andreevi,*

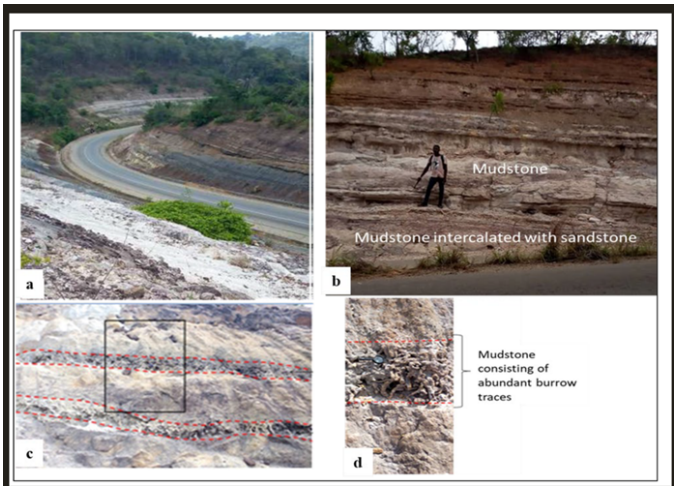

Figure 7. Road-cut sections within the study area: (a) an extensive road-cut section showing some of the exposed lithofacies; (b) road-cut section displaying some of the characteristic lithofacies; (c) road-cut exposure showing two layers of accumulated trace fossils with branching, vertical, and horizontal burrows (mainly *Thalassinoides*), where the two burrowed mudstone sub-facies are interbedded with mudstone sub-facies; (d) magnified view of the burrowed mudstone sub-facies showing filled burrow traces. Photograph (c) was taken along the Imiegba–Okpekpe Road (07°11′27.7″ N, 06°26′47.7″ E).

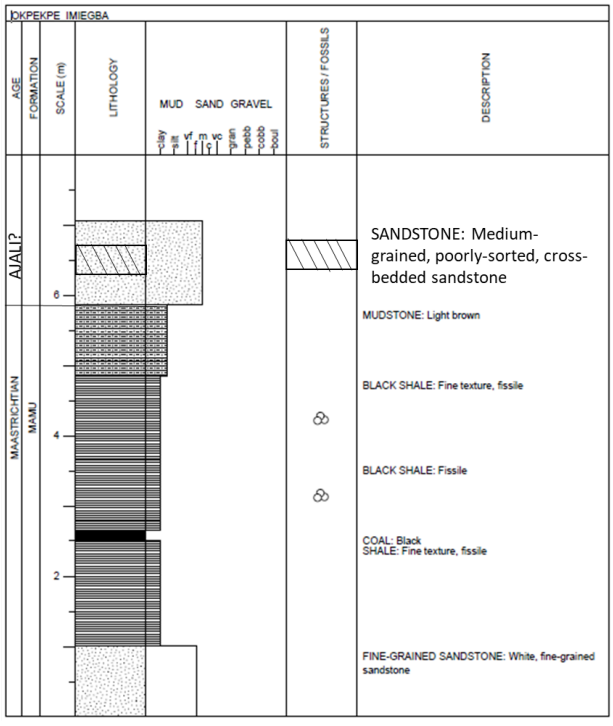

Figure 8. Lithologic section showing thick shale interbedded with a thin coal layer observed along the Imiegba and Okpekpe roads (07°12′00″ N, 06°28′00″ E).

Cyclonephelium Laevigatosporites major, *Odontochitina operculata*, and *Longapertites marginatus* [35, 36], Table 4). There-

Table 1. Textural characteristics of the sandstone facies associated with the Mamu Formation.

S#	Mz (ϕ)	σ_1 (ϕ)	SK1	KG	Interpretations
L7	0.30	1.28	0.08	2.35	Coarse-grained, poorly-sorted, near-symmetrical, very leptokurtic sandstone
L7B	1.06	1.60	-0.11	1.21	Medium-grained, poorly-sorted, coarse-skewed, leptokurtic sandstone
L7D	1.56	1.09	-0.11	1.36	Medium-grained, poorly-sorted, coarse-skewed, leptokurtic sandstone
L7E	1.24	0.08	-0.13	1.18	Medium-grained, very well-sorted, coarse-skewed, leptokurtic sandstone
L8A	1.07	0.95	-0.11	1.33	Medium-grained, moderately-sorted, coarse-skewed, leptokurtic sandstone.
L8B	0.3	1.00	0.07	1.07	Coarse-grained, moderately-sorted, nearly symmetrical, mesokurtic sandstone
L8D	0.35	1.35	0.05	2.24	Coarse-grained, poorly-sorted, nearly symmetrical, very leptokurtic sandstone
L8E	1.02	0.92	-0.14	1.27	Medium-grained, moderately-sorted, coarse-skewed, leptokurtic sandstone.
L9B	2.04	0.52	0.16	2.24	Fine-grained, moderately well-sorted, fine-skewed, very leptokurtic sandstone
L9C	0.56	2.42	0.05	0.84	Coarse-grained, very poorly-sorted, nearly symmetrical, platykurtic sandstone
L10A	1.47	1.07	-0.13	1.00	Medium-grained, poorly-sorted, coarse-skewed, mesokurtic sandstone
L10B	1.63	0.08	0.23	0.64	Medium-grained, very well-sorted, fine-skewed, very platykurtic sandstone
L10D	1.42	0.09	0.06	1.40	Medium-grained, very well-sorted, nearly symmetrical, leptokurtic sandstone
L11B	0.68	1.10	0.08	1.08	Coarse-grained, poorly-sorted, nearly symmetrical, mesokurtic sandstone
L11D	0.56	2.28	0.04	1.04	Coarse-grained, very poorly-sorted, nearly symmetrical, mesokurtic sandstone
Min.	0.30	0.08	-0.14	0.64	Coarse-grained, very well-sorted, coarse-skewed, very platykurtic sandstone
Max.	2.04	2.42	0.23	2.35	Fine-grained, very poorly-sorted, fine-skewed, very leptokurtic sandstone
Ave.	1.02	1.60	0.01	1.35	Medium-grained, poorly-sorted, nearly symmetrical, leptokurtic Sandstone

fore, from the extracted palynomorphs in the shale facies of the study section, the Early Maastrichtian age has been assigned to it. Most of the recovered palynomorphs have been reported in shale and mudstone sections by some of the earlier authors who worked on the Mamu Formation in the Benin Flank [16], and in the basin centre [6, 10, 37, 38]. Some of the analysed samples, however, contain combinations of palynomorphs that range in age from Late Cretaceous to Cenozoic. Such combinations may probably be a result of contamination during submarine downslope movement of younger materials to be merged with older sediment on the continental slope and canyon walls.

4.4. *Palaeoenvironment of the study area (Mamu Formation)*

The palaeoenvironmental reconstruction for the Mamu Formation is based on evidence from facies association and palynomorph associations.

4.4.1. *Palaeoenvironment via bivariate plots*

The bivariate plots obtained from the statistical parameters of the grain size analysis carried out on the sandstone facies showed that most of the sandstone was deposited in a fluvial (river) environment; some analysed sandstone fell on the beach field (Figure 15).

4.4.2. *Palaeoenvironments via discriminant functions*

Sahu [31] and [30] proposed certain formulas used to discriminate sedimentation within two similar depositional environments (e.g., Aeolian vs Beach; shallow marine vs Beach; Fluvial (Deltaic) vs Shallow marine, and Turbidity vs Fluvial (Deltaic). Following Sahu [30, 31], Y_1 (see equation (1)) was applied to infer Aeolian vs Beach (if the Y_1 value is less than -2.7411 or greater than -2.7411, respectively). The linear discrimination function revealed that over 93% and 7% of the sandstone were deposited in beach and aeolian deposits, respectively (Table 5). The Y_2 (equation (2)) values (based on Y_2 value

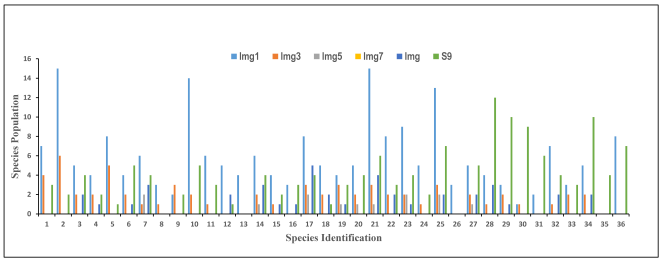

Figure 9. Species population of the Dinoflagellates obtained from the five different locations. Species identification numbers are as presented in Table 2.

< or > 65.3650 representing beach vs shallow agitated marine environments, respectively) suggest that about 80% and 20% of the sandstones of the studied sections accumulated in shallow marine and beach environmental settings, respectively. The Y_3 function (see equation (3)) was applied to distinguish between sedimentation in fluvial (beach) when Y_3 value is less than -7.4190 and shallow marine when Y_3 is greater than -7.4190. The Y_3 values suggested that 60% of the sediments were in fluvial (beach) while the remaining 40% were deposited in shallow marine environments. The Y_4 values (equation (4)) showed that 80% of the sandstones were deposited by turbidity current, while about 20% accumulated in a fluvial (deltaic) environment. This is because most of the sandstones have Y_4 values less than the threshold value of 9.8433 (i.e., turbidite), while a few of the sandstones have Y_4 values greater than the threshold value (i.e., fluvial deltaic deposits) (Table 5).

The multivariant discriminant functions, $\tilde{V}1$ and $\tilde{V}2$, were computed for the sandstone facies using equations (5) and (6) and tabulated (Table 6). The $\tilde{V}1$ and $\tilde{V}2$ values were plotted on a binary plot to infer environments of deposition for the analysed sandstones. The $\tilde{V}1$ versus $\tilde{V}2$ plot shows that about 40% fall

Table 2. Taxonomic distribution of the dinoflagellate cysts.

	Palynomorphs	Sample #						
Sample ID	Dinoflagellate cysts	Img1	Img3	Img5	Img7	Img	S9	Total
1	*Cleistosphaeridium diversispinosum*	07	04	-	-	-	03	14
2	*Trichodinium castaneum*	15	06	-	-	-	02	23
3	*Subtilisphaera pirnaensis*	05	02	-	-	02	04	13
4	*Spongodinium delitiense*	04	02	-	-	01	02	09
5	*Spiniferites ramosus*	08	05	-	-	-	01	14
6	*Senegalinium dubium*	04	02	-	-	01	05	12
7	*Senegalinium bicavatum*	06	01	02	-	03	04	16
8	*Palaeoperidinium pyrophorum*	03	01	-	-	-	-	04
9	*Palaeoperidinium cretaceum*	02	03	-	-	-	02	07
10	*Palaeohystrichophora infusorioides*	14	02	-	-	-	05	21
11	*Odontochitina porifera*	06	01	-	-	-	03	10
12	*Odontochitina operculata*	05	-	-	-	02	01	08
13	*Michrystridium piliferum*	04	-	-	-	-	-	04
14	*Isabelidinium sp.*	06	02	01	-	03	04	16
15	*Fibradinium annetorpense*	04	01	-	-	01	02	08
16	*Dinogymnium sp.*	03	-	-	-	01	03	07
17	*Cyclonephelium sp.*	08	03	02	-	05	04	22
18	*Cribroperidinium exilicristatum*	05	02	-	-	02	01	10
19	*Circulodinium distinctum*	04	03	01	-	01	03	12
20	*Cerodinium sp. A*	05	02	01	-	-	04	12
21	*Cerodinium obliquipes*	15	03	01	-	04	06	29
22	*Cerodinium diebelii*	08	02	-	-	02	03	15
23	*Cerodinium striatum*	09	02	02	-	01	04	18
24	*Cerodinium leptoderma*	05	01	-	-	-	02	08
25	*Areoligera coronata*	13	03	02	-	02	07	27
26	*Andalusiella gabonensis*	03	-	-	-	-	-	03
27	*Alterbidinium pilosum*	05	02	01	-	02	05	15
28	*Andalusiella polymorpha*	04	01	-	-	03	12	20
29	*Andalusiella mauthei*	03	02	-	-	01	10	16
30	*Apteodinium crassus*	01	01	-	-	-	09	11
31	*Batiacasphaera solida*	02	-	-	-	-	06	08
32	*Cyclonephelinium compactum*	07	01	-	-	02	04	14
33	*Cyclonephelium deconinckii*	03	02	-	-	-	03	08
34	*Palaeocystodinium golzowense*	05	02	-	-	02	10	19
35	*Pterodinium cornutum*	-	-	-	-	-	04	04
36	Foraminiferal test lining	08	-	-	-	-	07	15
Species Population		209	64	13	00	41	145	472
Species Diversity		35	29	09	00	20	33	

on the turbidite, 20% aeolian, 20% river, 13% shallow marine, and 7% beach fields (Figure 16). The results of both discriminatory analyses suggest that the sandstone facies of the studied sections were deposited in fluvial, shallow water, and beach settings. These further depict sediment accumulation under a mixed or transitional environment.

4.4.3. *Palaeoenvironmental reconstruction through facies evidence*

The facies association of the shale, mudstone, sandstone, and coal in Okpekpe, Imiegba, and surrounding areas suggest that they belong to a different lithostratigraphic unit from the Ajali Sandstone, which many authors considered as comprising mainly cross-bedded sandstone occurring in Auchi and Fugar areas [42]. Similar facies associations in the basin centre have been mapped as the Mamu Formation, which underlies thickly cross-bedded sandstone facies of the Ajali Sandstone [3, 23]. The road-cut section observed at Location 9 (along the roads to Okpekpe and Imiegba communities, Figure 8) also displays a similar scenario of cross-bedded sandstone (probably Ajali Sandstone) overlying intercalations of shale and mudstone (i.e., part of the Mamu Formation).

The lamination of the shale facies is evidence of floodplain or backwash. The shale beds generally decrease in thickness from bottom to top, and this suggests an upward-shallowing of the environment. The *Thalassinoides* ichnogenus of the mud-

Table 3. Taxonomic distribution of the spores and pollens in the shale facies of the Mamu Formation.

Palynomorphs		Sample #						
Species ID	Spores and Pollens	Img1	Img3	Img5	Img7	Img	S9	Total
1	*Verrucatosporites usmensis*	07	02	-	-	01	02	12
2	*Triplanosporites microsinuosus*	05	01	02	01	03	08	20
3	*Syndesmicopites typicus*	03	-	-	-	-	05	08
4	*Retibrevitricolpites triangulates*	04	-	-	-	-	-	04
5	*Pediculisporis microgranulatus*	03	02	-	-	02	03	10
6	*Monocolpites marginatus*	03	03	01	01	03	-	11
7	*Matonisporites equiexinus*	13	05	02	02	05	06	33
8	*Longapertites vandenbergi*	05	02	-	-	-	03	10
9	*Longapertites marginatus*	10	04	02	01	03	13	33
10	*Leiotriletes adriennis*	20	03	03	02	05	12	45
11	*Laevigatosporites major*	05	10	04	03	02	05	29
12	*Expressipollis calciferus*	05	-	-	-	-	-	05
13	*Retidiporites magdalenensis*	07	02	-	-	-	05	14
14	*Ericipites pachyexinus*	10	-	-	-	-	03	13
15	*Echitriporites triangulariformis*	14	05	-	-	03	06	28
16	*Cyathidites australis*	05	08	04	03	04	04	28
17	*Constructipollenites infectus*	09	03	01	-	02	06	21
18	*Cingulatisporites ornatus*	10	02	01	01	03	05	22
19	*Buttinia andreevi*	05	01	-	-	-	02	08
20	*Azolla cretacea*	02	-	-	-	01	-	03
21	*Ariadnaesporites nigeriensis*	03	01	-	-	-	02	06
22	*Aquilapollenites sp.*	05	02	-	-	01	03	11
23	*Syncolporites subtilis*	02	01	-	-	02	07	12
24	*Foveotriletes margaritae*	-	02	-	-	01	04	07
25	*Proteacidites obanji*	03	07	-	-	02	02	14
26	*Psilamonocolpites sp.*	08	25	02	01	01	03	40
27	*Laevigatosporites discordatus*	05	12	04	02	06	02	31
28	*Distaverrusporites simplex*	04	02	-	-	02	03	11
Species Population		175	107	26	17	52	114	491
Species Diversity		27	23	11	10	20	24	

Table 4. Age and depositional environment of some of the index markers (dinoflagellates, pollens, and spores) associated with the shale facies of the study area.

Age	Depth (m)	Location	Index marker assemblage (Dinoflagellate, Spores and Pollens)	Depositional environment [35, 36].
Early Maastrichtian	6.0	L7	*Dinogymnium sp., Longapertites marginatus*	Marine to terrestrial
	5.0	L8a	*Odontochitina operculata*	Marine to terrestrial
	3.0	L8b	*Cyclonephelium, laevigatos porites major*	Marine to terrestrial
	1.0	L10a	*Cerodinium diebelii, Buttinea andreevi Andahisiella polymorpha.*	Marine to terrestrial
	1.5	L10b	Cingulatisporites ornatus	Marine to terrestrial
	1.2	L11	*Trichodinum lasstaneum*	Marine to terrestrial

stone facies suggests possible deposition in a littoral (i.e., shallow marine) environment. The associated coal seam is indicative of deposition in a vegetated swampy environment. The overall facies associations that make up the studied sections therefore suggest sediment accumulation in a transitional environment between marine and non-marine environments, as attested to by Adedosu *et al*. [43] from studies of coal samples (obtained from Okaba and Onyeama Mines) from the Mamu Formation in the eastern part of the basin.

4.4.4. Palaeoenvironmental reconstruction via palynostratigraphic evidence

Spores and Pollen are generally the reproductive cells of vascular land plants that are often carried by wind or water and deposited in lakes, lagoons and marine environments. The index marker palyno-fauna (Dinoflagellates) and palyno-flora (Spores and Pollen) microfossils extracted from the analysed shales (Figures 10, 11, 13 and 14) are suggestive of sedimentation in a marine to terrestrial environment. However, an association of the Spores and Pollen with other marine microfos-

Table 5. Results of the linear discriminant function computed for the sandstone facies of the studied sections.

Sample #	Linear discriminant functions				Environment of deposition			
	Y_1	Y_2	Y_3	Y_4	Y_1	Y_2	Y_3	Y_4
L7	12.10	157.30	-14.55	12.50	Beach	Shallow Marine	Fluvial (Beach)	Fluvial (Deltaic)
L7B	9.69	205.20	-21.53	5.40	Beach	Shallow Marine	Fluvial (Beach)	Turbidity
L7D	3.29	125.70	-09.36	7.10	Beach	Shallow Marine	Fluvial (Beach)	Turbidity
L7E	-0.46	39.31	0.99	6.26	Beach	Beach	Shallow Marine	Turbidity
L8A	3.89	98.67	-7.00	6.71	Beach	Shallow Marine	Fluvial (Beach)	Turbidity
L8B	5.82	91.47	-8.966	5.95	Beach	Shallow Marine	Shallow Marine	Turbidity
L8D	12.40	167.60	-16.00	11.70	Beach	Shallow Marine	Fluvial (Beach)	Fluvial (Deltaic)
L8E	3.74	92.55	-6.38	6.17	Beach	Shallow Marine	Shallow Marine	Turbidity
L9B	0.36	94.05	-2.46	14.30	Beach	Shallow Marine	Shallow Marine	Fluvial (Deltaic)
L9C	22.20	410.00	-51.35	2.83	Beach	Shallow Marine	Fluvial (Beach)	Turbidity
L10A	2.38	114.40	-8.93	5.02	Beach	Shallow Marine	Fluvial (Beach)	Turbidity
L10B	5.25	111.60	-10.75	6.26	Beach	Shallow Marine	Fluvial (Beach)	Turbidity
L10D	-0.80	49.75	0.11	8.83	Beach	Beach	Shallow Marine	Turbidity
L11B	5.25	111.60	-10.75	6.26	Beach	Shallow Marine	Fluvial (Beach)	Turbidity
L11D	20.40	370.30	-45.53	4.08	Beach	Shallow Marine	Fluvial (Beach)	Turbidity

Note: Y_1 is used to discriminate between Beach and Aeolian deposits; Y_2 distinguish between Shallow marine and Beach environments; Y_3 differentiate between Fluvial (beach) and Shallow marine; Y_4 = Turbidity currents versus Fluvial (deltaic).

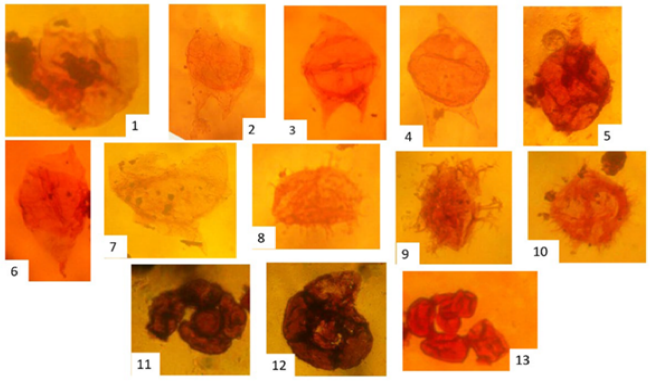

Figure 10. Photomicrographs of selected dinoflagellate cysts from the Mamu Formation: (1) *Cyclonephelium* sp., (2) *Cerodinium diebelii*, (3) *Cerodinium striatum*, (4) *Cerodinium obliquipes*, (5) *Pterodinium cornutum*, (6) *Isabelidinium* sp., (7) *Cyclonephelinium compactum*, (8) *Cleistosphaeridium diversispinosum*, (9) *Areoligera coronata*, (10) *Palaeohystrichophora infusoroides*, and (11–13) foraminiferal test linings (×40).

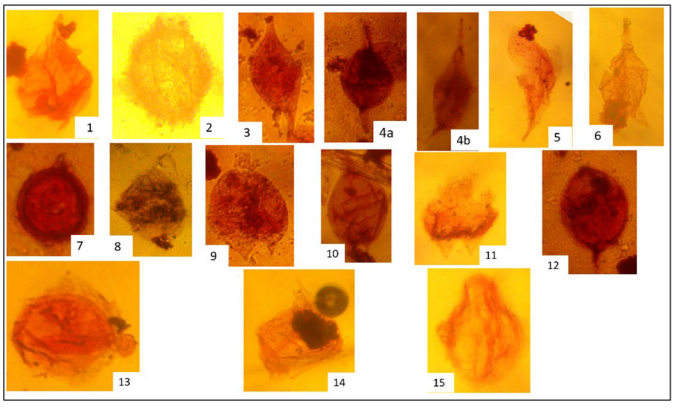

Figure 11. Continuation of Figure 10. Photomicrographs of selected dinoflagellate cysts from the Mamu Formation: (1) *Spongodinium delitiense*, (2) *Trichodinium castaneum*, (3) *Andalusiella polymorpha*, (4a, b) *Palaeocystodinium golzowense*, (5) *Odontochitina operculata*, (6) *Cerodinium leptoderma*, (7) *Apteodinium crassus*, (8, 14) *Alterbidinium pilosum*, (9, 11) *Senegalinium bicavatum*, (10) *Cerodinium obliquipes*, (12) *Andalusiella mauthei*, (13) *Subtilisphaera pirnaensis*, and (15) *Fibradinium annetorpense* (×40).

sils such as the Dinoflagellates (Table 2) and the Foraminifera lining (Figure 10) suggests that a marine condition prevailed during the deposition of the shale facies.

The Early Maastrichtian Mamu Formation can be thought to be deposited as a marine condition was setting in (shown by the littoral setting of the *Thalassinoides* ichnogenus of the mudstone facies, as well as the microfossil association of the palynomorphs and the Foraminiferal lining). The Mamu Formation could have been deposited in a transitional setting between non-marine (evidenced from the interbedded sandstone and coal facies) and marine (demonstrated by the microfossil Dinoflagellates and Foraminiferal lining) environments.

5. Conclusion

The facies associations (i.e., shale, mudstone, sandstone, and coal facies) in Okpekpe, Imiegba and environs are closely related to the lithostratigraphic unit described as the Mamu Formation in the Anambra Basin, southeastern Nigeria, where the basin centre occurs.

The age of the index marker microfossils extracted from the shale in this study (i.e., Dinoflagellates, Pollen and Spores) suggests an Early Maastrichtian for the studied litho-sections.

Bivariate plots, linear discriminant analysis using the statistical parameters obtained from grain-size analysis of the sand-

Table 6. Results of the multivariant discriminant function (Eigen vector $\tilde{V}1$ and $\tilde{V}2$) computed for the sandstone facies of the Mamu Formation.

Sample #	Mz (ϕ)	$\sigma(\phi)$	Sk_1	K_G	$\tilde{V}1$	$\tilde{V}2$	Environment
L7	0.3	1.28	0.08	2.35	2.24	1.31	Aeolian
L7B	1.06	1.60	-0.11	1.21	2.60	0.08	Turbidite
L7D	1.56	1.09	-0.11	1.36	2.05	0.96	Aeolian
L7E	1.24	0.08	-0.13	1.18	1.07	1.27	Beach
L8A	1.07	0.95	-0.11	1.33	1.62	0.95	Beach
L8B	0.30	1.00	0.07	1.07	1.27	0.52	Beach
L8D	0.35	1.35	0.05	2.24	2.32	1.14	Aeolian
L8E	1.02	0.92	-0.14	1.27	1.52	0.91	Beach
L9B	2.04	0.52	0.16	2.24	2.21	2.28	Shallow marine
L9C	0.56	2.42	0.05	0.84	4.31	-1.84	Not discriminated
L10A	1.47	1.07	-0.13	1.00	1.81	0.65	Beach
L10B	1.63	0.08	0.23	0.64	1.16	0.97	Beach
L10D	1.42	0.09	0.06	1.40	1.33	1.53	Beach
L11B	0.68	3.64	0.08	1.08	1.59	0.53	Beach
L11D	0.56	2.28	0.04	1.04	3.98	-1.37	Not discriminated

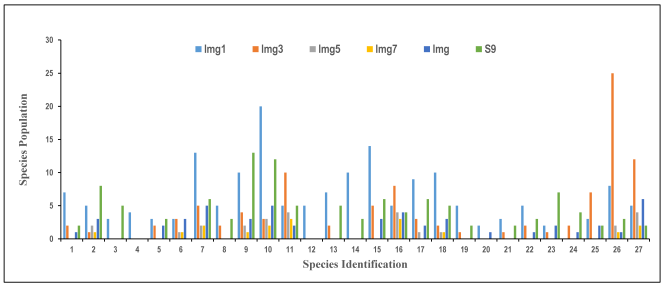

Figure 12. Species population of the Spores and Pollens grains obtained at five different locations. Species identification numbers are as presented in Table 3.

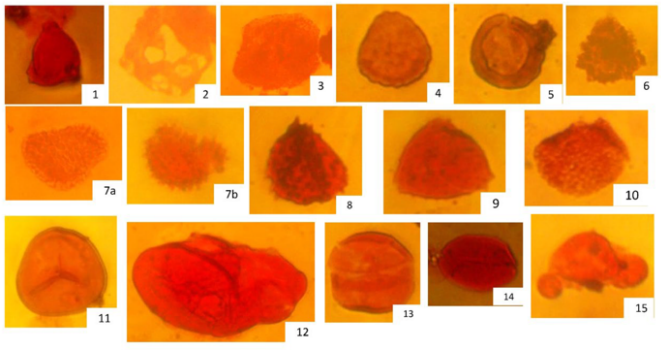

Figure 13. Photomicrographs of selected pollen and spores from the Mamu Formation: (1) *Proteacidites dehaani*, (2) *Buttinea andreevi*, (3) *Retidiporites magdalenensis*, (4) *Distaverrusporites simplex*, (5) *Cingulatisporites ornatus*, (6) *Retibrevitricolpites triangulatus*, (7a, b) *Constructipollenites ineffectus*, (8, 9) *Echitriporites trianguliformis*, (10) *Verrucatosporites usmensis*, (11) *Leiotriletes adriennis*, (12) *Longapertites vanendeenburgi*, (13) *Monocolpites marginatus*, (14) *Psilamonocopites* sp., and (15) *Pediculisporis microgranulatus* (×40).

stone facies of the Mamu Formation, all point to deposition in fluvial, beach, and shallow marine environments.

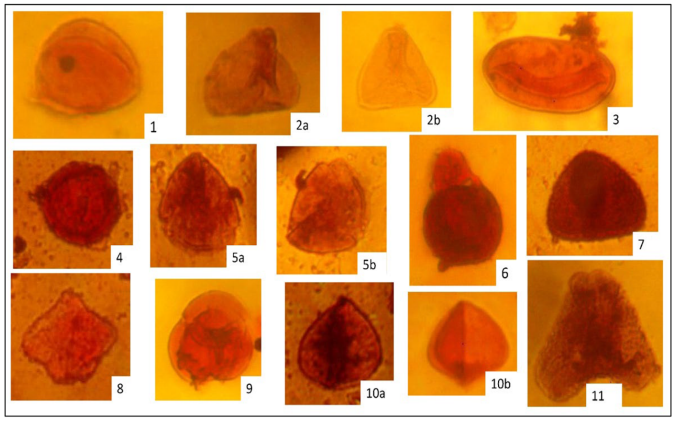

Figure 14. Continuation of Figure 13. Photomicrographs of selected pollen and spores from the Mamu Formation: (1) *Longapertites marginatus*, (2a, b) *Matonisporis equiexinus*, (3) *Laevigatosporites major*, (4) *Cingulatisporites ornatus*, (5a, b) *Syncolporites subtilis*, (6) *Ariadnaesporites nigeriensis*, (7) *Foveotrlletes margaritae*, (8) *Aquilapollenites* sp., (9) *Ericipites pachyexinus*, (10a, b) *Triplanossporites microsinuosus*, and (11) *Syndemicolpites typicus* (×40).

The facies analysis of the Mamu Formation favours deposition in a transitional environment. Palynostratigraphically, the association of palynomorphs is indicative of deposition in a shallow marine environment.

Data availability

The data used in this study were generated by the authors through geological fieldwork and laboratory analyses. All data supporting the findings of this study are available from the corresponding author upon reasonable request.

References

[1] C. S. Nwajide & T. J. A. Reijers, "Geology of southern Anambra Basin", in *Selected chapters on geology, sedimentary geology and sequence*

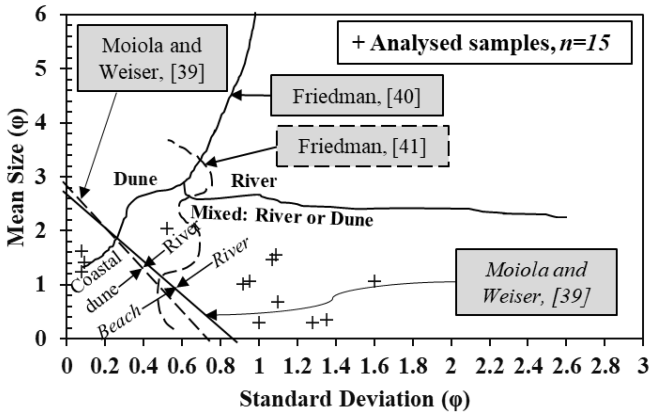

Figure 15. Bivariate plots of mean size versus standard deviation of the sandstone facies of the Mamu Formation (modified after Refs. [39–41]).

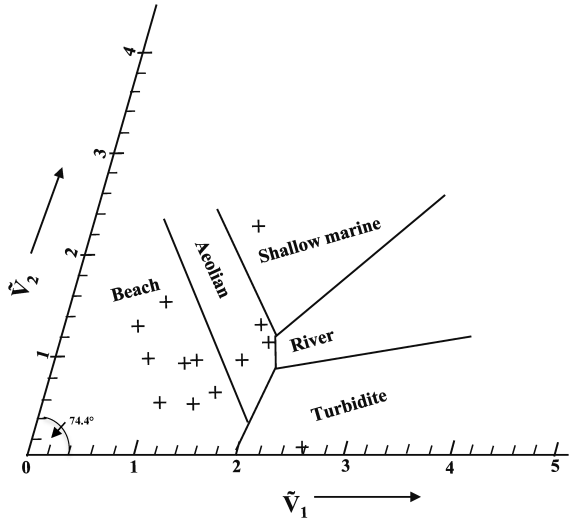

Figure 16. Bivariate plot of $\tilde{V}_1$ against $\tilde{V}_1$ (modified after Sahu [30]).

stratigraphy in Nigeria and three case studies and a field guide, T. J. A. Reijers (Ed.), SPDC Corporate Reprographic Services, Warri, Nigeria, 1996, p. 131.

[2] C. S. Nwajide, *Geology of Nigeria's sedimentary basins*, 1st ed., CSS Bookshops Ltd., Lagos, Nigeria, 2013, pp. 1–565.

[3] C. S. Nwajide, *Geology of Nigeria's sedimentary basins*, 2nd ed., Albishara Educational Publications, Enugu, Nigeria, 2022, pp. 349–445. https://virtuall.nln.gov.ng/resource/NLN-XAHR16DM8PVRJL6.

[4] I. M. Akaegbobi, J. I. Nwachukwu & M. Schmitt, "Aromatic hydrocarbon distribution and calculation of oil and gas volumes in post-Santonian shale and coal, Anambra Basin, Nigeria", in *Petroleum systems of South Atlantic margins*, M. R. Mello & B. J. Katz (Eds.), American Association of Petroleum Geologists Memoir 73, 2000, 233. https://doi.org/10.1306/M73705C17.

[5] S. O. Akande, I. B. Ogunmoyero, H. I. Petersen & H. P. Nytoft, "Source rock evaluation of coals from the lower Maastrichtian Mamu Formation, SE Nigeria", Journal of Petroleum Geology **30** (2007) 303. https://doi.org/10.1111/j.1747-5457.2007.00303.x.

[6] J. E. Ogala, O. A. Ola-Buraimo & M. I. Akaegbobi, "Palynological and palaeoenvironmental study of the Middle–Upper Maastrichtian Mamu coal facies in Anambra Basin, Nigeria", World Applied Sciences Journal **7** (2009) 1566. https://www.idosi.org/wasj/wasj7(12)/18.pdf.

[7] A. Adedosu, O. O. Sonibare, O. Ekundayo & J. Tuo, "Hydrocarbon-generative potential of coal and interbedded shale of Mamu Formation, Benue Trough, Nigeria", Petroleum Science and Technology **28** (2010) 412. https://doi.org/10.1080/10916460902725306.

[8] M. Abubakar, "Petroleum potentials of the Nigerian Benue Trough and Anambra Basin: a regional synthesis", Natural Resources **5** (2014) 25. https://doi.org/10.4236/nr.2014.51005.

[9] M. A. Adeleye, C. Y. Ugboaja & L. Yuhong, "Aspects of the hydrocarbon potential of the coals and associated mudstones and shales of the Mamu Formation in Anambra Basin, Nigeria", Journal of Environment and Earth Science **7** (2017) 1. https://www.iiste.org/Journals/index.php/JEES/article/view/37710.

[10] J. N. Chukwuma-Orji, E. A. Okosun, J. C. Ekom & J. F. Abolarin, "A palynology and paleoenvironmental study of a section from the Amansiodo-1 well, Anambra Basin, southeastern Nigeria", Geology, Geophysics and Environment **43** (2017) 293. https://doi.org/10.7494/geol.2017.43.4.293.

[11] C. I. P. Dim, K. M. Onuoha, I. C. Okwara, I. A. Okonkwo & P. O. Ibemesi, "Facies analysis and depositional environment of the Campano–Maastrichtian coal bearing Mamu Formation in the Anambra Basin, Nigeria", Journal of African Earth Sciences **152** (2019) 69. https://doi.org/10.1016/j.jafrearsci.2019.01.011.

[12] A. J. Edegbai, L. Schwark & F. E. Oboh-Ikuenobe, "Campano–Maastrichtian paleoenvironment, paleotectonics and sediment provenance of western Anambra Basin, Nigeria: multi-proxy evidences from the Mamu Formation", Journal of African Earth Sciences **156** (2019) 203. https://doi.org/10.1016/j.jafrearsci.2019.04.001.

[13] J. E. Ogala, "Depositional conditions of the Upper Cretaceous shales from the Anambra Basin, SE Nigeria: constraints from mineralogy and geochemistry", Journal of African Earth Sciences **196** (2022) 104670. https://doi.org/10.1016/j.jafrearsci.2022.104670.

[14] O. I. Ejeh, I. A. A. Etobro, K. Perleros, J. E. Ogala, A. O. Ehinola, K. Christanis & S. Kalaitzidis, "Hydrocarbon generation potential of Campano–Maastrichtian to Paleogene shales in the Benin Flank of the Anambra Basin, SW Nigeria", Energy Geoscience **5** (2024) 100286. https://doi.org/10.1016/j.engeos.2024.100286.

[15] K. K. Okeke, H. Slimani, H. Jbari, N. Ukpabi & A. N. Asadu, "Palynostratigraphy and palaeoenvironment of the Danian sediments from the Nsukka Formation of the Anambra Basin at the vicinity of Ikpankwu, southeastern Nigeria", Journal of African Earth Sciences **210** (2024) 105133. https://doi.org/10.1016/j.jafrearsci.2023.105133.

[16] O. Odedede, "Palaeopalynology and sequence stratigraphy of the Mamu Formation around Orhua, southwestern Nigeria", Nigerian Journal of Science and Environment **12** (2013) 128. https://doi.org/10.5987/UJ-NJSE.17.106.1.

[17] O. F. Adebayo, A. O. Ola-Buraimo, H. Y. Madukwe & A. O. Aturamu, "Palynological and sequence stratigraphy characterization of the Early–Late Campanian Nkporo Shale, Okpekpe–Imiegba area, Anambra Basin, Nigeria", European Journal of Basic and Applied Sciences **2** (2015) 1. https://www.idpublications.org/ejbas-vol-2-no-1-2015/.

[18] O. I. Ejeh, "The Maastrichtian sedimentary successions of the Anambra Basin recently exposed around Okpekpe and Imiegba: part of the Mamu or Ajali Formation?", Nigerian Journal of Science and Environment **14** (2016) 38. https://doi.org/10.5987/UJ-NJSE.16.056.1.

[19] A. O. Jayeola, A. O. Oluwajana, O. A. Olatunji, M. U. Udofia & O. Danjuma, "Sedimentological, palynological and foraminiferal biostratigraphic studies of the Upper Cretaceous Mamu Formation at Imiegba, Anambra Basin, Edo State, Nigeria", Achievers Journal of Scientific Research **1** (2016) 37. https://achieversciencejournal.org/ajosrojs/index.php/ajosr/issue/archive.

[20] S. O. Obaje, O. Akinyele, R. Ahmed, B. Alli & A. Adefemisoye, "Palynomorphs content and paleodepositional environments of Mamu Formation in Okpekpe-1, Imiegba-1 and Imiegba-2, Benin Flank of Anambra Basin, Nigeria", Journal of Applied Science, Environment and Management **26** (2022) 15. https://doi.org/10.4314/jasem.v26i9.13.

[21] C. A. Kogbe, "The Cretaceous and Paleogene sediments of southern Nigeria", in *Geology of Nigeria*, 2nd ed., C. A. Kogbe (Ed.), Rock-view (Nigeria) Limited, Jos, Nigeria, 1989, 325.

[22] A. Simpson, "The Nigerian coalfield: the geology of parts of Owerri and Benue Provinces", Bulletin of Geological Survey of Nigeria **24** (1954) 1. https://ngsa.gov.ng/publications-of-ngsa/.

[23] R. A. Reyment, *Aspect of the geology of Nigeria*, University of Ibadan Press, Ibadan, Nigeria, 1965, 145.

[24] Nigerian Geological Survey Agency (NGSA), "Geological map of Nigeria", Published by the authority of the Federal Republic of Nigeria, Abuja, Nigeria, 2006. https://ngsa.gov.ng/geological-maps/.

[25] U. A. Lar, T. P. Bata, H. U. Dibal, R. I. Daspan, L. C. Isah, A. A. Fube & D. A. Bassi, "Field, petrographic and geochemical study of basement, clastic and carbonate petroleum reservoirs in the northern Benue Trough, Nigeria", Petroleum Technology Development Journal **8** (2018) 36. https://www.ptdjournal.com/?page_id=8.

[26] M. I. Akaegbobi & M. Schmitt, "Organic facies, hydrocarbon source potentials and reconstruction of the depositional paleoenvironment of the Campano–Maastrichtian Nkporo Shale in the Cretaceous Anambra Basin, Nigeria", Nigerian Association of Petroleum Explorationists Bulletin **13** (1998) 1.

[27] G. O. Ogungbesan & T. A. Adedosu, "Geochemical record for the depositional condition and petroleum potential of the Late Cretaceous Mamu Formation in the western flank of Anambra Basin, Nigeria", Green Energy and Environment **5** (2020) 83. https://doi.org/10.1016/j.gee.2019.01.008.

[28] R. L. Folk & W. C. Ward, "Brazos River Bar: a study of the significance of grain-size parameters", Journal of Sedimentary Petrology **29** (1957) 3. https://doi.org/10.1306/74D70646-2B21-11D7-8648000102C1865D.

[29] B. K. Sahu, "Depositional mechanisms from the size analysis of clastic sediments", Journal of Sedimentary Research **34** (1964) 73. https://doi.org/10.1306/74D70FCE-2B21-11D7-8648000102C1865D.

[30] I. A. A. Etobro, O. I. Ejeh & G. O. Ovwamuedo, "Fluvial sedimentology of the River Ethiope sediments, Niger Delta, southern Nigeria", Rudarsko-geološko-naftni zbornik RGNZ/MGPB (The Mining–Geology–Petroleum Engineering Bulletin) **39** (2024) 45. https://doi.org/10.17794/rgn.2024.2.4.

[31] B. K. Sahu, "Multigroup discrimination of depositional environments using size distribution statistics", Indian Journal of Earth Sciences **10** (1983) 20.

[32] G. M. Friedman & J. E. Sanders, *Principles of sedimentology*, Wiley, New York (1978). https://www.researchgate.net/publication/268449121.

[33] J. S. Boggs, *Petrology of sedimentary rocks*, Cambridge University Press, Cambridge (2009). https://doi.org/10.1017/CBO9780511626487.

[34] C. Baiyegunhi, K. Liu & O. Gwavava, "Grain size statistics and depositional pattern of the Ecca Group sandstones, Karoo Supergroup in the Eastern Cape Province, South Africa", Open Geoscience **9** (2017) 554. https://doi.org/10.1515/geo-2017-0042.

[35] E. Schrank, "Organic-walled microfossils and sedimentary facies in the Abu Tartur Phosphate (Late Cretaceous), Egypt", Berliner geowissenschaftliche Abhandlungen, Reihe A **50** (1984) 177.

[36] G. L. Williams & J. P. Bujak, "Mesozoic and Cenozoic dinoflagellates", in H. M. Bolli, J. B. Saunders & K. Perch-Nielsen (eds.), *Plankton stratigraphy*, Cambridge University Press, Cambridge (1985) 847.

[37] C. G. Soronnadi-Ononiwu, A. O. Omoboriowo & N. V. Chukwujekwe, "Palynological and paleoenvironmental studies of the Mamu Formation, Enugu area, Anambra Basin, Nigeria", International Journal of Pure and Applied Sciences and Technology **10** (2012) 1.

[38] K. C. Chiadikobi, O. I. Chiaghanam, O. C. Onyemesili & A. O. Omoboriowo, "Palynological study of the Campano–Maastrichtian Nkporo Group of Anambra Basin, southeastern Nigeria", World News of Natural Sciences **20** (2018) 31. https://www.researchgate.net/publication/336303394.

[39] R. J. Moiola & D. Weiser, "Textural parameters: an evaluation", Journal of Sedimentary Petrology **38** (1968) 45. https://doi.org/10.1306/74D718C5-2B21-11D7-8648000102C1865D.

[40] G. M. Friedman, "The distinction between dune, beach, and river sands from their textural characteristics", Journal of Sedimentary Petrology **31** (1961) 514. https://doi.org/10.1306/74D70BCD-2B21-11D7-8648000102C1865D.

[41] G. M. Friedman, "Dynamic processes and statistical parameters for size-frequency distributions of beach and river sands", Journal of Sedimentary Petrology **37** (1967) 327. https://doi.org/10.1306/74D716CC-2B21-11D7-8648000102C1865D.

[42] N. I. Oronsaye, "Origin and depositional environments of the sandstone deposits in Fugar area, Bendel State, Nigeria", Nigerian Journal of Mining and Geology **4** (1987) 96.

[43] T. A. Adedosu, O. O. Sonibare, J. Tuo & O. Ekundayo, "The occurrence of lacustrine depositional setting in the Mamu Formation, Anambra Basin, Nigeria", Energy Sources, Part A: Recovery, Utilization and Environmental Effects **36** (2014) 374. https://doi.org/10.1080/15567036.2010.538801.